



RESEARCH ARTICLE OPEN ACCESS

PET/CT Imaging of the Right Heart Perfusion and Glucose Metabolism Depending on a Risk Status in Patients With Idiopathic Pulmonary Arterial Hypertension

Natalia Goncharova¹ | Daria Ryzhkova² | Kirill Lapshin³ | Anton Ryzhkov⁴ | Aryana Malanova² | Elizaveta Andreeva¹ | Olga Moiseeva¹

¹Department of Noncoronary Disease, Almazov National Medical Research Center, Saint Petersburg, Russia | ²Department of Nuclear Medicine and Radiology, Almazov National Medical Research Center, Saint Petersburg, Russia | ³Intensive Care Unit Department, Almazov National Medical Research Center, Saint Petersburg, Russia | ⁴Department of Magnetic Resonance Imaging, Almazov National Medical Research Center, Saint Petersburg, Russia

Correspondence: Natalia Goncharova (ns.goncharova@gmail.com)

Received: 6 August 2024 | **Revised:** 26 December 2024 | **Accepted:** 9 January 2025

Funding: The study was supported by the Russian Science Foundation (agreement number 23-15-00318).

Keywords: [13N]-ammonia PET/CT | [18F]-FDG PET/CT | idiopathic pulmonary arterial hypertension | metabolism | risk stratification

ABSTRACT

Right ventricular heart failure (RV HF) is the leading cause of death in pulmonary arterial hypertension (PAH). Relevance of the low-risk status assessment using available diagnostic tools requires a reliable confirmation. The study aimed to evaluate right ventricular perfusion and glucose metabolism using positron emission tomography (PET)/computed tomography (CT) with [13N]-ammonia and [18F]-fluorodeoxyglucose ([18F]-FDG) in 30 IPAH patients (33.8 ± 9.4 years) according to ESC/ERS 2022 risk status. The ratio of SUVmax_{RV/LV} metabolism and SUVmax_{RV/LV} perfusion showed significant positive correlation with pulmonary artery pressure, right heart dilatation, NT-proBNP level and negative correlation with the RV ejection fraction. The SUVmax_{RV/LV} perfusion and SUVmax_{RV/LV} metabolism ratios differed significantly according to risk status. Low risk patients had a SUVmax_{RV/LV} metabolism comparable to the controls without PH. The SUVmax_{RV/LV} perfusion ratio was elevated in low-risk IPAH patients compared with controls. Increased SUVmax_{RV/LV} perfusion may be an early marker of coronary flow adaptation to RV pressure overload in low-risk IPAH patients and requires further evaluation. Further long-term studies are needed to determine the clinical relevance and cut-off values for the RV/LV PET/CT with [13N]-ammonia and [18F]-fluorodeoxyglucose ([18F]-FDG) uptake in different IPAH risk groups.

1 | Introduction

Idiopathic pulmonary arterial hypertension (IPAH) is a rapidly progressive disease with high mortality due to the right ventricular heart failure (RV HF) [1]. Right ventricle-pulmonary artery coupling varies substantially [2] and determines survival in IPAH patients. Patients with IPAH who exhibit long-term vasoreactivity provide the best example of significant decrease

in pulmonary arterial pressure (PAP), sustained maintenance of low-risk status, and the highest survival among all PAH patients [3]. However, PAP normalization does not occur in the vast majority of IPAH patient with negative vasoreactive test (VRT-) with PAH-specific therapy, even with low risk status [4]. According to the guideline low risk status does not require further escalation of PAH specific therapy [5]. While the 3-year survival is 78.4% (73.1%–82.9%) in patients with WHO

This is an open access article under the terms of the [Creative Commons Attribution-NonCommercial](https://creativecommons.org/licenses/by-nc/4.0/) License, which permits use, distribution and reproduction in any medium, provided the original work is properly cited and is not used for commercial purposes.

© 2025 The Author(s). *Pulmonary Circulation* published by John Wiley & Sons Ltd on behalf of Pulmonary Vascular Research Institute.

functional Class I–II PAH at baseline [6]. The validated risk assessment tools ESC/ERS 2022 [5] and REVEAL [7] may be insufficient to reliably describe the disease state and prognosis in low-risk IPAH patients. The assessment of the RV myocardial perfusion and glucose metabolism using molecular imaging may identify an early RV–PA uncoupling and may assist in a decision-making to escalate PAH-specific therapy prior to clinical manifestation.

The study aimed to evaluate right ventricle myocardial perfusion and glucose metabolism depending on risk status in IPAH patients.

2 | Methods

2.1 | Data Collection

The inclusion criteria into the study were defined as a mean mean PAP ≥ 25 mmHg, pulmonary capillary wedge pressure (PCWP) < 15 mmHg and pulmonary vascular resistance (PVR) ≥ 3 Wood units. Pulmonary arterial compliance (PAC) was calculated with parameters derived from the right heart catheterization (RHC): stroke volume/(systolic pulmonary artery pressure–diastolic pulmonary artery pressure) [5]. The exclusion criteria for the study were defined as PAH other etiologies than IPAH, moderate to severe lung disease; left heart disease; established malignancies; diabetes mellitus; thyroid disease; severe kidney or liver dysfunction, inflammatory diseases and mental disorders.

Demographics, symptoms, 6-min walk test (6MWT) distance, cardiac magnetic resonance imaging (MRI) and positron emission tomography/computed tomography (PET/CT) with two radiopharmaceuticals [^{13}N]-ammonia and [^{18}F]-fluorodeoxyglucose ([^{18}F]-FDG), laboratory values (hemoglobin, creatinine with estimated glomerular filtration rate [eGFR], N-terminal pro-brain-type natriuretic peptide [NT-proBNP]) were collected at a baseline through 1 month when RHC was performed. Estimated GFR was calculated according to the CKD-EPI equation. Cardiac MRI was done using MAGNETOM Trio A Tim Sistem 3 Tesla (Siemens, Germany). All patients underwent RHC, echocardiography, MRI, PET/CT, NT-proBNP and 6MWT at the time of study conduction. VRT with inhaled Iloprost (Bayer, Germany) carried out in 27 patients as a part of the RHC. Positive VRT was defined as previously described [5, 8, 9]. ESC/ERS 2022 baseline 3-strata risk stratification was performed [<https://www.pahinitiative.com/hcp/risk-assessment/calculators>] (URL accessed on June, 01 2024) in all patients at the time of study conduction. The following variables were used for ESC/ERS 2022 risk calculation: symptoms (edema, syncope, and progression), PAH functional class (WHO), 6MWT, NT-proBNP, echocardiography variables (right atrial area, tricuspid annular plane systolic excursion/systolic PAP, and pericardial effusion), cardiac MRI variables (RV end-systolic volume index, stroke volume index, and RV ejection fraction), invasive hemodynamic variables (mean right atrial pressure, cardiac index, stroke volume index, and mixed venous oxygen saturation).

2.2 | PET/CT Protocol

PET/CT («Discovery 710», GE Healthcare, USA) with [^{18}F]-FDG and [^{13}N]-ammonia was performed in all patients in

two separate days. Myocardial glucose metabolism was assessed with [^{18}F]-FDG PET/CT as radiopharmaceutical. Patients fasted at least 6 h before the procedure [^{18}F]-FDG PET/CT. A standard dose of 5 MBq/kg (< 550 MBq) of [^{18}F]-FDG was injected intravenously 1 h after an insulin-euglycemic clamp, when stable glycemia was established (optimal glycemia was 5 mmol/L). Plasma glucose levels were checked every 5 min. Static [^{18}F]-FDG PET/CT imaging was started in 40 min after tracer injection to ensure accurate myocardial uptake of the tracer. Low dose CT was performed for attenuation correction. PET/CT perfusion images were acquired at rest according to a standard protocol with [^{13}N]-ammonia. Immediately after the CT transmission scan, static PET perfusion images were acquired in 5 min after intravenous administration of 10 MBq/kg [^{13}N]-ammonia.

The areas of the left ventricle (LV) and RV myocardial uptake were identified visually on the static transaxial images. The regions of interest (ROI) drawn on the RV free wall, and LV lateral wall (Figure 1). The maximal standardized uptake value (SUVmax) was obtained in each ROIs using software AWS 4.6 (GE Healthcare, USA). The ratio of SUVmax RV free wall and SUVmax LV lateral wall was calculated for both [^{18}F]-FDG and [^{13}N]-ammonia PET images for assessment of glucose metabolism (SUVmax_{RV/LV} metabolism) and perfusion (SUVmax_{RV/LV} perfusion) of the RV myocardium. The SUVmax_{RV/LV} metabolism/SUVmax_{RV/LV} perfusion ratio was calculated for evaluation the relationship between perfusion and metabolism in the right heart myocardium. The control group for PET/CT study comprised of six patients without cardiorespiratory pathology and normal estimated systolic PAP on echocardiography, age and gender comparable with the study cohort. RHC and cardiac MRI were not performed in the control group without pulmonary hypertension, as there were no indications.

The study was conducted in accordance with the Declaration of Helsinki and approved by the Ethics Committee of the Almazov National Medical Research Centre of the Ministry of Health of the Russian Federation, (protocol N 04-23, approved on April 17, 2023). Informed consent was obtained from all subjects participating in the study. Written informed consent was obtained from the patient(s) for publication of this paper.

2.3 | Study Population

The study population comprised 30 (18–52 years old) Caucasian IPAH patients (Table 1) prospectively recruited in a single-PH referral center between February 2020 and April 2024. The study included IPAH patients with positive VRT. Positive VRT was registered in 13 patients and negative VRT—in 14 patients. VRT was not performed in three patients with IV FC in accordance with the guidelines. No one patient dropped from the analysis. The entire cohort was divided into three groups based on ESC/ERS 2022 risk status: low-risk ($n = 6$), intermediate risk ($n = 18$), and high risk ($n = 6$). Twenty-four incident patients underwent initial PAH diagnostics and were treatment naïve.

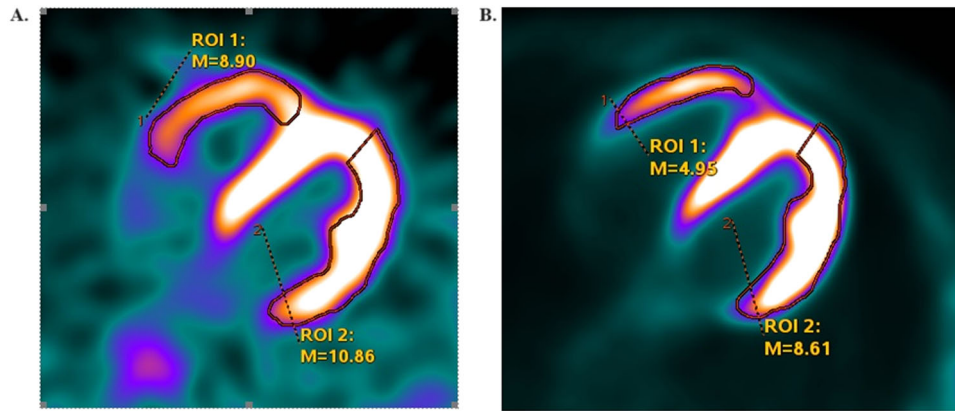


FIGURE 1 | SUV calculation methodology for radiopharmaceuticals: (A) Transaxial positron emission tomography (PET) image with [13N]-ammonia. (B) Transaxial PET image with [18F]-fluorodeoxyglucose ([18F]-FDG). The regions of interest (ROI) are drawn on the free wall of the right ventricle and the lateral wall of the left ventricle.

Six patients were prevalent. They enrolled into the study within 6–12 months from the initial diagnosis of IPAH in the center. All study procedures (RHC, MRI, NT-proBNP, 6MWT, and clinical assessment) were performed in the prevalent patients at the time of study and the risk stratification was calculated using ESC/ERS 2022 risk score based on the obtained parameters. Among prevalent patients, four VRT+ patients received CCB therapy at the time of the study. Two III–IV FC (WHO) patients received triple combination therapy including macitentan, sildenafil, and inhaled iloprost.

2.4 | Statistical Analysis

Demography, clinical data including PAH functional class (FC) (WHO), smoking, hemodynamic data, laboratory, MRI and PET/CT parameters were compared in three risk groups. Numerical parameters with a normal distribution were presented as mean \pm standard deviation ($M \pm SD$), and numerical parameters with an abnormal distribution presented as median and interquartile range (IQR; $M \pm 25\%$, 75%). Categorical variables presented as absolute numbers and percentages and compared using Fisher exact or Pearson M-L Chi-square tests, as appropriate. Mean values compared using the unpaired *t*-Student test and analysis of variance, as appropriate. Correlations were evaluated using the Pearson's correlation analysis. A statistically significant difference determined as a two-tailed $p < 0.05$. The statistical analyses of the data carried out using Statistica for Windows, version 10.0 (StatSoft: Tulsa, Okla, USA).

3 | Results

3.1 | 2022 ESC/ERS Risk Status

Patients in the three risk groups were comparable in age, body mass index, smoking, hemoglobin concentration and lung function test (Table 1). Low-risk group was represented with VRT+ patients and signs of mild pulmonary vascular disease (mean PAP of 30.8 ± 8.3 mmHg and PVR of 3.9 (3.1 ; 5.4) Wu), NT-proBNP within the reference range and mild right heart

remodeling. The intermediate and high-risk groups differed significantly from the low risk patients in hemodynamic and MRI parameters, 6MWT and NT-proBNP level, FC (WHO) (Table 1). There was no significant difference in mean PAP ($p = 0.3$), RAP and PAC values ($p = 0.08$; $p = 0.08$, respectively) between the intermediate and high-risk groups.

3.2 | PET/CT Imaging

The lowest $SUV_{max_{RV/LV}}$ metabolism and $SUV_{max_{RV/LV}}$ perfusion registered in patients with low ESC/ERS 2022 risk status compared with the intermediate/high risk IPAH patients. No difference was revealed in $SUV_{max_{RV/LV}}$ metabolism between the low risk patients and controls without PH (Table 2, Figure 2). $SUV_{max_{RV/LV}}$ perfusion was significantly higher in low-risk IPAH patients compared to the controls without PH (Table 2, Figure 3). The lowest $SUV_{max_{RV/LV}}$ perfusion observed in low-risk patients, and significantly differed from the intermediate/high risk groups. No significant difference registered ($p = 0.9$) in $SUV_{max_{RV/LV}}$ perfusion between the intermediate and high-risk patients (Figure 3). The ratio of $SUV_{max_{RV/LV}}$ metabolism and $SUV_{max_{RV/LV}}$ perfusion significantly differed between all risk groups with the highest value in the high-risk patients (Table 2, Figure 4).

3.3 | PET/CT Correlation in Entire IPAH Cohort

Significant positive correlations revealed between the $SUV_{max_{RV/LV}}$ metabolism and RV volumes, mean PAP, PVR, NT-proBNP, and negative correlations with CI, PAC, and RV ejection fraction. Significant positive correlation was determined between the $SUV_{max_{RV/LV}}$ perfusion and RV dilatation, mean PAP, PVR, PAC, and NT-proBNP (Table 3). The value of $SUV_{max_{RV/LV}}$ metabolism correlated with $SUV_{max_{RV/LV}}$ perfusion ($r = 0.65$, $p = 0.0001$) (Figure 5). Positive correlations registered between $SUV_{max_{RV/LV}}$ metabolism/ $SUV_{max_{RV/LV}}$ perfusion ratio and mean PAP, PVR, RV end-systolic volume index, NT-proBNP level, and negative correlations with cardiac index and RV ejection fraction (Table 3).

TABLE 1 | Characteristics of IPAH patients depending on ESC/ERS 2022 risk status.

Parameters, <i>n</i> (%); <i>m</i> ± <i>SD</i> ; <i>M</i> , <i>IQR</i> ; 25;75.	Entire cohort, <i>n</i> = 30	Low risk, <i>N</i> = 6	Intermediate risk, <i>N</i> = 18	High risk, <i>N</i> = 6	<i>p</i> -value, *, **, ***
Age (years)	33.9 ± 9.4	29.5 ± 6.5	35.2 ± 10.0	34.3 ± 10.0	0.2; 0.8; 0.3
Male, <i>n</i> (%)	2 (6.7)	1 (16.7)	1 (5.6)	0	n/a
BMI (kg/m ²)	25.2 ± 6.9	23.2 ± 3.7	26.5 ± 8.0	23.2 ± 4.8	0.3; 0.3; 0.9
Smoking, <i>n</i> (%)	6 (20)	2 (33.3)	2 (11)	2 (33.3)	0.3
Prevalent, <i>n</i> (%)	6 (20)	4 (66.6)	0	2 (33.3)	n/a
VRT+, <i>n</i> (%)	13 (43.3)	6 (100)	7 (38.9)	0	0.03
Functional class (WHO)					
FC III–IV, <i>n</i> (%)	19 (63.3)	0	13 (72.2)	6 (100)	0.03
Exercise test					
6MWT, m	379.7 ± 123.8	487.3 ± 78.5	384.9 ± 96.5	256.3 ± 137.2	0.03; 0.02; 0.005
Laboratory parameters					
NT-proBNP, pg/mL	893 (165; 3087)	55.5 (46.2; 68.0)	893.0 (453.7; 1495.0)	5447.0 (4836.0; 6089.0)	0.01; < 0.001; < 0.0001
eGFR, mL/min/1.73m ²	94.6 ± 28.2	99.2 ± 30.5	98.7 ± 25.8	77.7 ± 31.4	0.9; 0.1; 0.2
Hemoglobin, g/L	142.1 ± 18.5	137.3 ± 15.2	144.4 ± 21.0	140.2 ± 14.5	0.4; 0.6; 0.7
Lung function test					
FVC, %	94.0 ± 19.7	103.2 ± 24.8	93.5 ± 19.1	86.6 ± 15.0	0.3; 0.4; 0.2
FEV1, %	85.7 ± 16.3	98.9 ± 22.2	83.5 ± 12.0	79.0 ± 16.7	0.04; 0.4; 0.1
DLCO, %	73.2 ± 16.8	77.9 ± 16.1	73.9 ± 16.0	66.4 ± 20.5	0.6; 0.4; 0.3
RHC					
mBP, mmHg	85.5 ± 11.8	91.8 ± 18.5	84.8 ± 9.3	81.2 ± 9.9	0.2; 0.4; 0.2
mPAP, mmHg	56.0 ± 20.8	30.8 ± 8.3	60.1 ± 17.4	68.8 ± 20.1	0.0007; 0.3; 0.002
RAP, mmHg	7.3 ± 5.3	3.8 ± 2.6	7.1 ± 4.1	11.5 ± 8.0	0.08; 0.08; 0.05
PCWP, mmHg	8.1 ± 3.5	7.2 ± 4.8	7.7 ± 3.3	10.2 ± 1.7	0.7; 0.09; 0.1
CI, L/min/m ²	2.4 ± 0.7	3.3 ± 0.7	2.3 ± 0.6	1.8 ± 0.3	0.002; 0.03; 0.0002
PVR, WU	12.0 (7.1; 17.8)	3.9 (3.1; 5.4)	12.0 (10.5; 15.5)	24.2 (14.8; 34.7)	0.009; 0.03; 0.0006
Sat O ₂ , %	95.4 ± 2.6	97.6 ± 1.1	95.2 ± 2.6	93.8 ± 2.4	0.04; 0.2; 0.005
SvO ₂ , %	61.4 ± 12.6	75.4 ± 4.1	62.0 ± 8.5	45.8 ± 11.2	0.001; 0.001; 0.0001
PAC, mL/mmHg	1.5 ± 1.0	2.8 ± 0.7	1.3 ± 0.8	0.7 ± 0.4	0.0007; 0.08; 0.00005
MRI					
RA short dimension, mm	50.1 ± 10.2	41.3 ± 4.5	51.4 ± 8.1	55.7 ± 14.6	0.009; 0.4; 0.04
RV EDV index, mL/m ²	82.1 ± 18.6	68.1 ± 12.3	81.7 ± 17.7	97.3 ± 15.9	0.1; 0.07; 0.005
RV ESV index, mL/m ²	55.4 ± 17.8	36.0 ± 8.0	55.2 ± 11.6	75.4 ± 17.8	0.001; 0.0005; 0.0006
RV wall thickness, mm	6.2 ± 1.9	4.7 ± 1.5	6.3 ± 1.7	7.5 ± 1.9	0.06; 0.1; 0.02
RV EF, %	35.8 ± 11.5	46.8 ± 7.0	36.6 ± 8.9	22.5 ± 8.6	0.02; 0.003; 0.0003
LA short dimension, mm	28.4 ± 4.8	32.3 ± 5.3	28.2 ± 4.5	25.0 ± 2.3	0.08; 0.1; 0.01

(Continues)

TABLE 1 | (Continued)

Parameters, <i>n</i> (%); <i>m</i> ± SD; <i>M</i> , IQR; 25;75.	Entire cohort, <i>n</i> = 30	Low risk, <i>N</i> = 6	Intermediate		<i>p</i> -value, *, **, ***
			risk, <i>N</i> = 18	High risk, <i>N</i> = 6	
LV EDV index, mL/m ²	57.6 ± 15.4	71.1 ± 11.0	59.0 ± 12.8	40.5 ± 9.3	0.05; 0.004; 0.0004
LV ESV index, mL/m ²	22.9 ± 7.5	28.0 ± 7.0	22.4 ± 7.1	19.1 ± 7.2	0.1; 0.3; 0.05
LV SV index, mL/m ²	35.0 ± 10.2	43.4 ± 5.5	36.9 ± 8.1	21.4 ± 3.5	0.08; 0.0002; 0.000009
LV EF, %	61.0 ± 4.7	60.6 ± 6.0	62.2 ± 4.4	58.2 ± 3.4	0.5; 0.06; 0.4
RV EDVi/LV EDVi	1.4 (1.0; 1.9)	0.93 (0.91; 1.0)	1.4 (1.2; 1.6)	2.5 (1.8; 2.9)	0.01; 0.0008; 0.001
RV ESVi/LV ESVi	2.4 (1.5; 3.6)	1.3 (1.3; 1.4)	2.6 (1.9; 3.3)	4.2 (2.8; 4.4)	0.04; 0.02; 0.01
PAH therapy					
CCB, <i>n</i> (%)	4 (13.3)	3 (50%)	1 (5.5)	0	n/a
Sildenafil, <i>n</i> (%)	2 (6.6)	0	0	2 (33.3)	n/a
Macitentan, <i>n</i> (%)	2 (6.6)	0	0	2 (33.3)	n/a
Iloprost inhaled, <i>n</i> (%)	2 (6.6)	0	0	2 (33.3)	n/a

Note: *Difference between low and intermediate risk groups; **difference between intermediate and high risk group; ***difference between low and high risk groups. Abbreviations: [18 F]-FDG, 18F-Fluorodeoxyglucose; [13 N]-NH₃, ammonia; BMI, body mass index; CI, cardiac index; CCB, calcium channel blockers; DLCO, diffusion capacity of the lungs for carbon monoxide; EDVi, end-diastolic volume index; ESVi, end-systolic volume index; eGFR, estimated glomerular filtration rate; EF, ejection fraction; ESC, European Society of Cardiology; ERS, European Respiratory Society; FC, functional class; FEV₁, forced expiratory volume in one second; FVC, forced vital capacity; IPAH, Idiopathic pulmonary arterial hypertension; LA, left atrial; LV, left ventricle; max, maximal; mBP, mean blood pressure; mPAP, mean pulmonary artery pressure; MRI, magnetic resonance imaging; n/a, not applicable; NT-proBNP, N-terminal pro-brain-type natriuretic peptide; PAC, pulmonary artery compliance; PCWP, pulmonary capillary wedge pressure; PET, positron emission tomography; PVR, pulmonary vascular resistance; RA, right atrial; RAP, right atrial pressure; RHC, right heart catheterization; RV, right ventricle; Sat O₂, arterial oxygen saturation; SV, stroke volume; SUV, standardized uptake value; SvO₂, mixed venous oxygen saturation; 6MWT, 6 min walk test.

4 | Discussion

For the first time, differences in [18F]-FDG and [13N]-NH₃ right ventricle myocardial uptake according to ESC/ERS 2022 risk status were identified in IPAH patients. The advantage of the study was a pure IPAH population without comorbidities, mostly untreated, a short period between all studies and the presence of a control group. While the limited number of patients with different etiologies of PAH may confound the results of PET/CT [10–12]. The etiology of PAH modifies the hemodynamic characteristics and myocardial structure with extremely high RV myocardial mass in congenital heart defect-PAH [13, 14] and myocardial stiffness in scleroderma [15]. High number of IPAH patients with positive VRT was the feature of our study. They had mild pulmonary vascular disease and formed the majority of the low-risk group.

Myocardial dysfunction, metabolism and perfusion are tightly interconnected [16]. The assessment of RV/LV myocardial metabolism in combination with myocardial perfusion was another advantage of our study. Bokhari et al. [17] evaluated [18F]-FDG and [13N]-NH₃ uptake in 16 prevalent IPAH I-II FC (WHO) patients. The correlations between the RV/LV [18F]-FDG uptake ratio and mean PAP, and between the RV/LV [13N]-NH₃ uptake ratio and mean PAP were similar to our data and subsequent studies [18–23]. There was no control group and no correlations reported between cardiac MRI and PET imaging in Bokhari et al [17] study. We derived the ratio between RV/LV

myocardial metabolism and the RV/LV myocardial perfusion in an attempt to reflect a physiological set of metabolic-perfusion relationships. The SUVmax_{RV/LV} metabolism and SUVmax_{RV/LV} perfusion ratio demonstrated significant positive correlation with pulmonary artery pressure, right heart dilatation, NT-proBNP level and negative correlation with the RV ejection fraction derived from MRI in IPAH patients. We did not find significant correlation between the RV metabolism, perfusion and 6MWT distance, which was inconsistent with other studies [19, 24]. Better hemodynamic profile, smaller right heart volume, low NT-proBNP level and higher exercise tolerance were recorded in patients with low-risk compared to the intermediate-high risk groups. RV [18F]-FDG uptake was comparable in low risk patients and non-PH controls and was clearly lower than in the intermediate/high risk groups. At the same time, SUVmax_{RV/LV} perfusion was significantly higher in low-risk patients compared to the control group. We assumed that an increase in RV myocardial blood flow supply adequately compensated RV metabolic demand in response to increased pressure load in low-risk patients. We observed a gradual increase in SUVmax_{RV/LV} metabolism from low-risk to high-risk patients, without corresponding magnification in RV perfusion in high-risk patients. This observation confirms the mismatch in RV supply–demand associated with the severity of PAH [25]. Indeed, decreased RV blood supply [26, 27] and reduced RV myocardial perfusion reserve [28, 29] have been confirmed in patients with severe PAP elevation, RV dysfunction and dilatation.

TABLE 2 | The RV/LV ratio [18F]-FDG and [13N]-NH3 uptake, hemodynamic and MRI data and ESC/ERS 2022 risk stratification in entire IPAH cohort ($n = 30$) and in control group without pulmonary hypertension.

Parameters	Controls without PH ($n = 6$)	Low risk ($n = 6$)	p -value between controls and low-risk	Intermediate risk ($n = 18$)	High risk ($n = 6$)	p -value*
[18F]-FDG uptake in heart						
SUVmaxRV/LV lateral wall	0.27 ± 0.07	0.38 ± 0.09	0.4	0.89 ± 0.27	1.2 ± 0.3	0.0002
[13N]-NH3 uptake in heart						
SUVmaxRV/LV lateral wall	0.42 ± 0.03	0.65 ± 0.06	0.0002	0.85 ± 0.15	0.79 ± 0.2	0.03
Metabolism/perfusion ratio of the RV/LV lateral wall						
SUVmax 18F-FDG/SUVmax [13N]-NH3	0.68 ± 0.26	0.69 ± 0.27	0.86	1.55 ± 0.67	2.56 ± 0.86	0.001
RHC						
mPAP, mmHg	n/a	30.8 ± 8.3	n/a	61.6 ± 18.8	65.5 ± 15.2	0.002
PVR, WU	n/a	4.1 ± 1.1	n/a	15.0 ± 8.9	25.9 ± 10.5	0.0013
PAC, mL/mmHg	n/a	2.84 ± 0.7	n/a	1.27 ± 0.83	0.67 ± 0.35	0.0002
MRI						
RVESVi, mL/m ²	n/a	35.9 ± 7.9	n/a	55.4 ± 11.1	84.5 ± 13.3	0.000001
RV EF, %	n/a	46.8 ± 6.9	n/a	35.7 ± 9.2	19 ± 3.6	0.0001
RVESVi/LVESVi	n/a	1.29 ± 0.1	n/a	2.7 ± 1.1	5.3 ± 3.1	0.0005
RV wall thickness, mm	n/a	4.6 ± 1.5	n/a	6.3 ± 1.8	8 ± 0.8	0.016

Note: *difference in between low risk and intermediate/high risk patients.

Abbreviations: [18 F]-FDG, 18F-Fluorodeoxyglucose; [13 N]-NH3, ammonia; EF, ejection fraction; ESVi, end-systolic volume index; IPAH, Idiopathic pulmonary arterial hypertension; LV, left ventricle; max, maximal; mPAP, mean pulmonary artery pressure; n/a, not applicable; PVR, pulmonary vascular resistance; PAC, pulmonary artery compliance; RV, right ventricle; SUV, standatized uptake value.

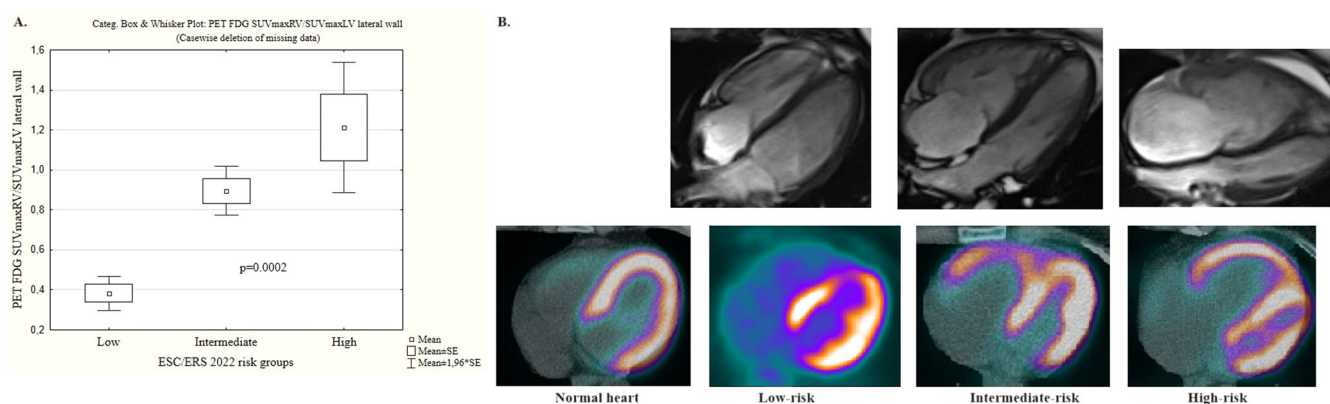
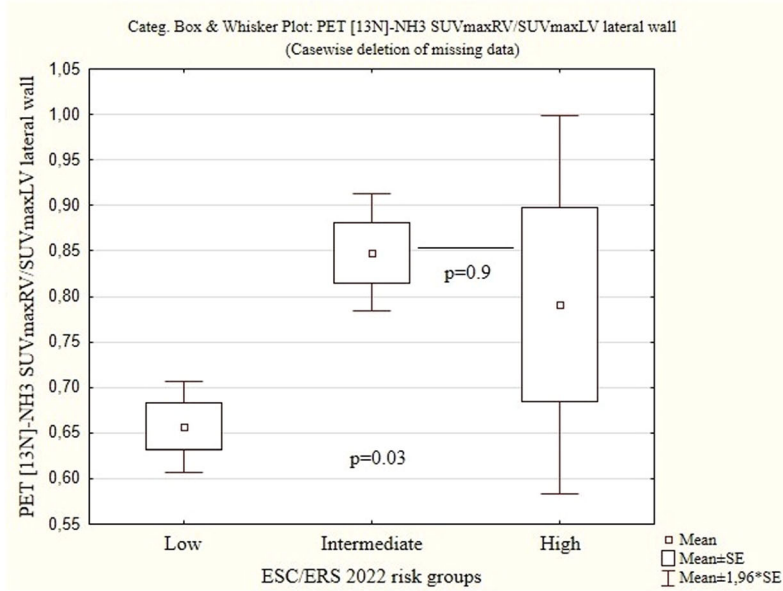


FIGURE 2 | Glucose metabolism and cardiac imaging according to risk status in IPAH patients ($n = 30$): (A) RV/LV lateral wall ratio of the maximal [18F]-FDG uptake. (B) Cardiac MRI and [18F]-FDG PET imaging. [18 F]-FDG, 18F-Fluorodeoxyglucose; IPAH, Idiopathic pulmonary arterial hypertension; LV, left ventricle; MRI, magnetic resonance imaging; PET, positron emission tomography; RV, right ventricle.

PET is an expensive diagnostic tool for assessing the severity of PAH. Glucose metabolism reflects the current energy deficient state and the transition to the anaerobic metabolic pathway due to the pressure and volume overload of the RV in patients with PAH. The question arises in which category of IPAH patients and for what purpose PET might be applied. Tatebe et al. [12] revealed that PET-FDG SUV adjusted for partial volume effect

(cRV-SUV) ≥ 8.3 was associated with time to clinical worsening (log-rank, $p = 0.0050$ and death ($p = 0.07$) in 27 PH patients. However, the PH group was heterogeneous: 9 patients with chronic thromboembolic pulmonary hypertension and three patients with portopulmonary hypertension, which may have influenced the patterns of right ventricle overload and the causes of death. Kazimjerczyk et al. [23] demonstrated that

A.



B.

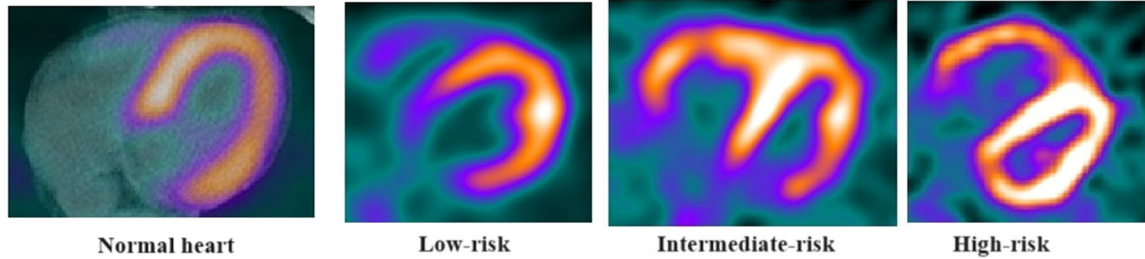


FIGURE 3 | Right ventricle ammonia uptake and PET imaging according to risk status in IPAH patients ($n = 30$): (A) RV/LV lateral wall ratio of the maximal [13N]-NH₃ uptake. (B) [13N]-Ammonia PET imaging of the heart in patients with low-, intermediate- and high-risk. IPAH, Idiopathic pulmonary arterial hypertension; LV, left ventricle; PET, positron emission tomography; RV, right ventricle.

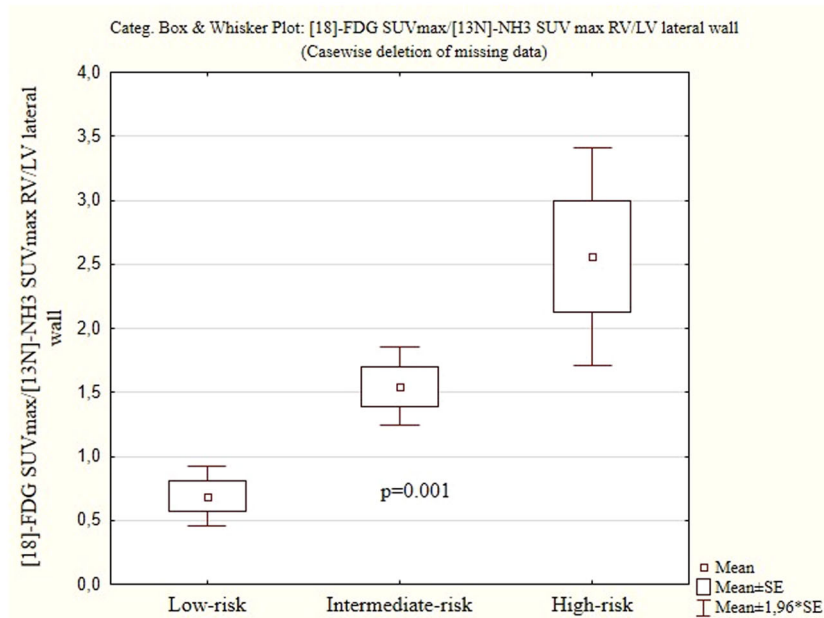


FIGURE 4 | RV/LV metabolism to perfusion ratio according to ESC/ERS 2022 risk status in the IPAH cohort. ESC, European Society of Cardiology; ERS, European Respiratory Society; IPAH, Idiopathic pulmonary arterial hypertension; LV, left ventricle; RV, right ventricle.

TABLE 3 | Correlations between the RV/LV lateral wall ratio of [18F]-FDG and [13N]-NH3 uptake, the ratio of RV/LV lateral wall metabolism to perfusion and hemodynamic, MRI, 6MWT, and laboratory parameters in entire IPAH cohort.

Parameters	[18 F]-FDG SUVmaxRV/LV lateral wall			[13 N]-NH3 SUVmaxRV/LV lateral wall			RV/LV [18 F]-FDG SUVmax/[13 N]-NH3 SUVmaxRV lateral wall		
	r	t	p	r	t	p	r	t	p
6MWT, m	−0.25	−1.3	0.2	−0.13	−0.7	0.5	−0.36	−1.9	0.06
NT-proBNP, pg/ml	0.67	4.6	0.00009	0.41	2.4	0.02	0.63	4.1	0.0003
RV ESVindex, ml/m2	0.71	4.8	0.00006	0.38	2.1	0.04	0.62	3.8	0.0007
RVESVi/LVESVi	0.72	5.1	0.00003	0.38	2.1	0.04	0.58	3.5	0.002
RV wall thickness, mm	0.72	5.0	0.00004	0.54	3.3	0.003	0.60	3.7	0.001
RV EF, %	−0.75	−5.6	0.00001	−0.43	−2.4	0.02	−0.68	−4.6	0.0001
mPAP, mmHg	0.61	3.9	0.0006	0.66	4.7	0.00006	0.51	3.0	0.006
CI, L/min/m ²	−0.72	−5.3	0.00001	−0.36	−2.1	0.047	−0.52	−3.1	0.004
PVR, WU	0.69	4.9	0.00005	0.50	3.1	0.004	0.52	3.2	0.003
PAC, mL/mmHg	−0.48	−2.8	0.009	−0.51	−3.2	0.004	−0.30	−1.6	0.1

Abbreviations: [18 F]-FDG, 18F-Fluorodeoxyglucose; [13 N]-NH3, ammonia; 6MWT, 6 min walk test; CI, cardiac index; EF, ejection fraction; ESVi, end-systolic volume index; IPAH, Idiopathic pulmonary arterial hypertension; LV, left ventricle; max, maximal; mPAP, mean pulmonary artery pressure; NT-proBNP, N-terminal pro-brain-type natriuretic peptide; PAC, pulmonary artery compliance; PVR, pulmonary vascular resistance; RV, right ventricle; SUV, standardized uptake value.

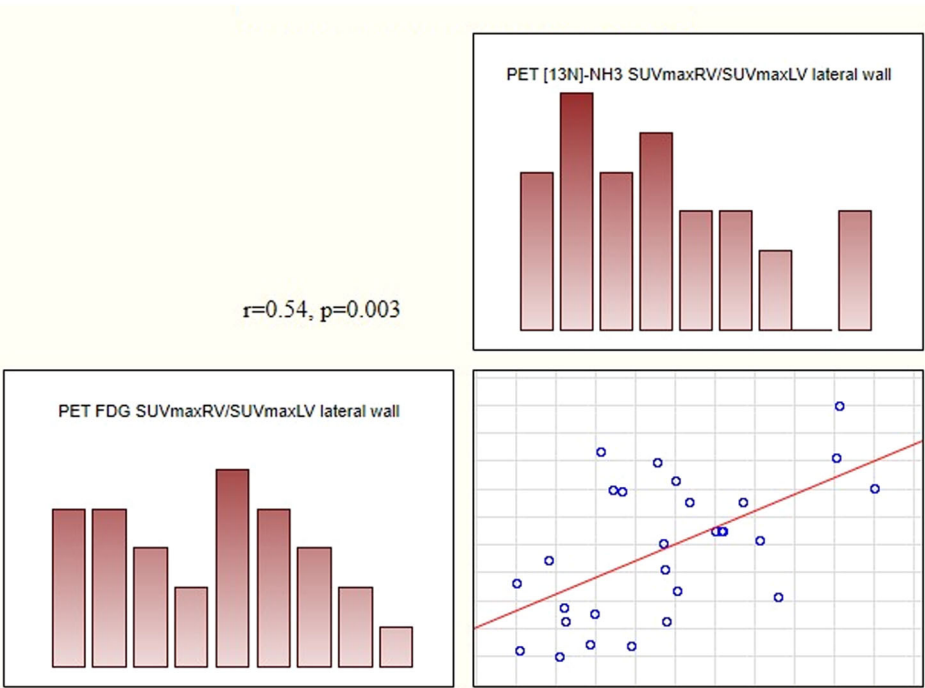


FIGURE 5 | Correlation between the RV/LV metabolism and perfusion in IPAH cohort. [13N]-NH3, ammonia; IPAH, Idiopathic pulmonary arterial hypertension; LV, left ventricle; PET, positron emission tomography; RV, right ventricle.

$SUV_{RV/LV} \geq 0.54$ by [18F]-FDG PET/CT was associated with decreased survival in PAH patients. According to that study $SUV_{maxRV/LV}$ metabolism decreased along with hemodynamic improvement with PAH specific therapy. These outcomes studies are of great importance. However, mean RV/LV ratios of [18F]-FDG and [13N]-NH3 uptake according to the risk status were not provided. Further studies with larger sample size and selected PAH etiology are needed to assess the diagnostic accuracy of the [18F]-FDG SUV RV/LV cut-off value.

The intermediate and high-risk patients typically have one or more non-invasive criteria consistent with the risk status (low exercise capacity, right heart dilatation and dysfunction on echocardiography or MRI, elevated NT-proBNP level). These data are sufficient to guide the decision on PAH therapy escalation. Thus, the use of PET/CT may be unnecessarily expensive in IPAH patients with the intermediate/high risk to guide therapy. While low risk patients remain in a “grey zone” of choosing PAH therapy numbers. The lack of benefit of initial

combination therapy compared to monotherapy in terms of PAH progression and survival was observed in low-risk PAH patients in AMBITION trial [30] and meta-analyses by Boucly et al. [31]. In the present study, the metabolic state of the RV myocardium in low-risk IPAH patients was similar to that of the control group without PH and cardiovascular diseases. This indicated a compensated state achieved by increasing RV myocardial perfusion in low-risk IPAH patients.

PET/CT in combination with invasive hemodynamic and MRI may support the definition of mild pulmonary vascular disease with adaptive RV remodeling and the true low-risk status in young IPAH patients. Investigation of the RV/LV metabolic-perfusion coupling using PET/CT may shed light on the intrinsic mechanism of the RV adaptation to the chronic overload and transition to decompensation state. Assessment of [18F]-FDG and [13N]-NH₃ uptake by the RV myocardium is particularly relevant in connection with the emergence of fundamentally new drugs, like sotatercept [32], mitochondrial [22, 32–34], or targeted RV myocardial vascularization therapy [25].

4.1 | Limitations

The hemodynamic criteria for PAH for the study were defined as mean PAP \geq 25 mmHg, PCWP $<$ 15 mmHg and PVR \geq 3 Wood units according to the national guidelines 2020 for the management of pulmonary hypertension [35]. The definition of PAH with mean PAP \geq 20 mmHg, PCWP $<$ 15 mmHg and PVR \geq 2 Wood units was introduced into clinical practice in September 2024 with the updated 2023 national guidelines for the management of pulmonary hypertension [36]. The absence of patients with negative VRT in the low-risk group may affect results of PET/CT, hemodynamics and cardiac remodeling indices. The small sample size of IPAH patients and the absence of long-term follow-up data did not allow for evaluation of PET/CT in terms of prognosis and PAH treatment effect. The metabolic/perfusion ratio was calculated based on [18F]-FDG and [13N]-ammonia PET/CT studies performed on two consecutive days.

5 | Conclusion

SUV_{maxRV/LV} metabolism/SUV_{maxRV/LV} perfusion ratio positively correlated with hemodynamic markers of pulmonary vascular disease severity, maladaptive RV remodeling, NTproBNP level and negatively correlated with RV systolic function in IPAH patients.

RV myocardial [18F]-FDG and [13N]-ammonia uptake varied significantly according to ESC/ERS 2022 risk status in young IPAH patients without comorbidity.

Comparable values of the SUV_{maxRV/LV} metabolism in low risk IPAH patients with controls without PH were associated with hemodynamic signs of mild pulmonary vascular disease, RV remodeling and compensatory increase of [13N]-ammonia myocardial accumulation.

5.1 | New Evidence from the Study

For the first time, RV/LV [18F]-FDG and [13N]-ammonia uptake values were characterized according to ESC/ERS 2022 risk status in IPAH patients.

Increased SUV_{maxRV/LV} perfusion may be an early marker of coronary blood flow adaptation to the RV pressure overload in IPAH patients with low-risk and requires further evaluation of its clinical relevance.

Author Contributions

Natalia Goncharova created the conception of the study, organized the database, performed statistical analysis and data interpretation, wrote the first draft of the manuscript, agreed to be accountable for all aspects of the work in ensuring that questions related to the accuracy or integrity of any part of the work are appropriately investigated and resolved. Daria Ryzhkova participated in conception of the study, performed and interpreted PET/CT studies, provided illustrations, and reviewed the manuscript. Olga Moiseeva participated in conception of the work, reviewed the manuscript and data interpretation, provide approval for publication of the content, and organized the study funding and performance. Kirill Lapshin performed right heart catheterization with vasoreactive testing, data interpretation, and reviewed the manuscript. Anton Ryzhkov performed cardiac MRI, provided illustrations, data interpretation, and reviewed the manuscript. Aryuna Malanova participated in PET/CT studies and data collection. Elizaveta Andreeva participated in data collection, manuscript preparation for submission. All authors contributed to manuscript revision, read, and approved the submitted version.

Acknowledgments

The authors thank Molokova Evgenia, MD and Orlova Galina, MD for the valuable participation in the PET/CT study conduction. This study was supported by the Russian Science Foundation, agreement number 23-15-00318.

Ethics Statement

The study was conducted in accordance with the Declaration of Helsinki, and approved by the Ethics Committee of the Almazov National Medical Research Centre, Ministry of Health of Russia, (protocol N 04-23, approved on April 17, 2023).

Consent

Informed consent was obtained from all subjects participating in the study. Written informed consent was obtained from the patient(s) for publication of this paper.

Conflicts of Interest

The authors declare no conflicts of interest.

Data Availability Statement

The data supporting the conclusions of this study are available from the corresponding author upon reasonable request.

References

1. A. Vonk Noordegraaf and N. Galiè, “The Role of the Right Ventricle in Pulmonary Arterial Hypertension,” *European Respiratory Review* 20, no. 122 (2011): 243–253.

2. R. R. Vanderpool, K. S. Hunter, M. Insel, et al., "The Right Ventricular-Pulmonary Arterial Coupling and Diastolic Function Response to Therapy in Pulmonary Arterial Hypertension," *Chest* 161, no. 4 (2022): 1048–1059.
3. F. Gerhardt, E. Fiessler, K. M. Olsson, et al., "Positive Vasoreactivity Testing in Pulmonary Arterial Hypertension: Therapeutic Consequences, Treatment Patterns, and Outcomes in the Modern Management Era," *Circulation* 149, no. 20 (2024): 1549–1564.
4. M. Ishiguro, K. Takeuchi, H. Kikuchi, et al., "Pulmonary Artery Pressure as a Treatment Target to Improve the Prognosis of Idiopathic Pulmonary Arterial Hypertension - Insight From a Cohort From Two Japanese Pulmonary Hypertension Centers," *Circulation Reports* 2, no. 4 (2020): 249–254.
5. M. Humbert, G. Kovacs, M. M. Hoeper, et al., "2022 ESC/ERS Guidelines for the Diagnosis and Treatment of Pulmonary Hypertension," *European Heart Journal* 43, no. 38 (2022): 3618–3731.
6. N. H. Kim, M. Fisher, D. Poch, C. Zhao, M. Shah, and S. Bartolome, "Long-Term Outcomes in Pulmonary Arterial Hypertension by Functional Class: A Meta-Analysis of Randomized Controlled Trials and Observational Registries," *Pulmonary Circulation* 10, no. 4 (2020): 2045894020935291.
7. R. L. Benza, M. Gomberg-Maitland, C. G. Elliott, et al., "Predicting Survival in Patients With Pulmonary Arterial Hypertension," *Chest* 156, no. 2 (2019): 323–337.
8. N. Nakanishi, et al., "2009 ESC/ERS Pulmonary Hypertension Guidelines and Connective Tissue Disease," *Allergology International* 60, no. 4 (2011): 419–424.
9. N. Galiè, M. Humbert, J. L. Vachiery, et al., "2015 ESC/ERS Guidelines for the Diagnosis and Treatment of Pulmonary Hypertension: The Joint Task Force for the Diagnosis and Treatment of Pulmonary Hypertension of the European Society of Cardiology (ESC) and the European Respiratory Society (ERS): Endorsed by: Association for European Paediatric and Congenital Cardiology (AEPC), International Society for Heart and Lung Transplantation (ISHLT)," *European Heart Journal* 37, no. 1 (2016): 67–119.
10. M. M. Can, C. Kaymaz, I. H. Tanboga, et al., "Increased Right Ventricular Glucose Metabolism in Patients With Pulmonary Arterial Hypertension," *Clinical Nuclear Medicine* 36, no. 9 (2011): 743–748.
11. T. Yang, L. Wang, C. M. Xiong, et al., "The Ratio of (18)F-FDG Activity Uptake between the Right and Left Ventricle in Patients With Pulmonary Hypertension Correlates With the Right Ventricular Function," *Clinical Nuclear Medicine* 39, no. 5 (2014): 426–430.
12. S. Tatebe, Y. Fukumoto, M. Oikawa-Wakayama, et al., "Enhanced [18F]fluorodeoxyglucose Accumulation in the Right Ventricular Free Wall Predicts Long-Term Prognosis of Patients With Pulmonary Hypertension: A Preliminary Observational Study," *European Heart Journal - Cardiovascular Imaging* 15, no. 6 (2014): 666–672.
13. G. P. Diller, K. Dimopoulos, H. Kafka, S. Y. Ho, and M. A. Gatzoulis, "Model of Chronic Adaptation: Right Ventricular Function in Eisenmenger Syndrome," *European Heart Journal Supplements* 9, no. suppl_H (2007): H54–H60.
14. R. J. Kameny, S. A. Datar, J. Boehme, et al., "The Adaptive Right Ventricle in Eisenmenger Syndrome: Potential Therapeutic Targets for Pulmonary Hypertension?," in *Molecular Mechanism of Congenital Heart Disease and Pulmonary Hypertension*, eds. T. Nakanishi, H. S. Baldwin, J. R. Fineman, H. Yamagishi (Singapore: Springer, 2020), 183–192.
15. L. A. Bissell, M. Y. Md Yusof, and M. H. Buch, "Primary Myocardial Disease in Scleroderma-A Comprehensive Review of the Literature to Inform the UK Systemic Sclerosis Study Group Cardiac Working Group," *Rheumatology* 56, no. 6 (2017): 882–895.
16. E. Schulz, S. Schuhmacher, and T. Münzel, "When Metabolism Rules Perfusion: Ampk-Mediated Endothelial Nitric Oxide Synthase Activation," *Circulation Research* 104, no. 4 (2009): 422–424.
17. S. Bokhari, A. Raina, E. Berman Rosenweig, et al., "PET Imaging May Provide a Novel Biomarker and Understanding of Right Ventricular Dysfunction in Patients With Idiopathic Pulmonary Arterial Hypertension," *Circulation: Cardiovascular Imaging* 4, no. 6 (2011): 641–647.
18. H. Ohira, R. deKemp, E. Pena, et al., "Shifts in Myocardial Fatty Acid and Glucose Metabolism in Pulmonary Arterial Hypertension: A Potential Mechanism for a Maladaptive Right Ventricular Response," *European Heart Journal - Cardiovascular Imaging* 17, no. 12 (2016): 1424–1431.
19. L. Wang, W. Li, Y. Yang, et al., "Quantitative Assessment of Right Ventricular Glucose Metabolism in Idiopathic Pulmonary Arterial Hypertension Patients: A Longitudinal Study," *European Heart Journal - Cardiovascular Imaging* 17, no. 10 (2016): 1161–1168.
20. D. Saygin, K. B. Highland, S. Farha, et al., "Metabolic and Functional Evaluation of the Heart and Lungs in Pulmonary Hypertension by Gated 2-[18F]-Fluoro-2-deoxy-D-glucose Positron Emission Tomography," *Pulmonary Circulation* 7, no. 2 (2017): 428–438.
21. W. Li, L. Wang, C. M. Xiong, et al., "The Prognostic Value of 18F-FDG Uptake Ratio Between the Right and Left Ventricle in Idiopathic Pulmonary Arterial Hypertension," *Clinical Nuclear Medicine* 40, no. 11 (2015): 859–863.
22. R. Kazimierczyk, P. Szumowski, S. G. Nekolla, et al., "Prognostic Role of PET/MRI Hybrid Imaging in Patients with Pulmonary Arterial Hypertension," *Heart* 107, no. 1 (2021): 54–60.
23. R. Kazimierczyk, P. Szumowski, S. G. Nekolla, et al., "The Impact of Specific Pulmonary Arterial Hypertension Therapy on Cardiac Fluorodeoxyglucose Distribution in PET/MRI Hybrid Imaging-Follow-Up Study," *EJNMMI Research* 13, no. 1 (2023): 20.
24. J. Osorio Trujillo, O. Tura-Ceide, J. Pavia, et al., "18-FDG Uptake on PET-CT and Metabolism in Pulmonary Arterial Hypertension," *Pulmonary Hypertension* 1 (2021): PA588.
25. V. Agrawal, T. Lahm, G. Hansmann, and A. R. Hemnes, "Molecular Mechanisms of Right Ventricular Dysfunction in Pulmonary Arterial Hypertension: Focus on the Coronary Vasculature, Sex Hormones, and Glucose/Lipid Metabolism," *Cardiovascular Diagnosis and Therapy* 10, no. 5 (2020): 1522–1540.
26. S. A. van Wolferen, J. T. Marcus, N. Westerhof, et al., "Right Coronary Artery Flow Impairment in Patients With Pulmonary Hypertension," *European Heart Journal* 29, no. 1 (2007): 120–127.
27. A. Hamud, M. Brezins, A. Shturman, A. Abramovich, and R. Dragu, "Right Coronary Artery Diastolic Perfusion Pressure on Outcome of Patients With Left Heart Failure and Pulmonary Hypertension," *ESC Heart Failure* 8, no. 5 (2021): 4086–4092.
28. J. Vogel-Claussen, J. Skrok, M. L. Shehata, et al., "Right and Left Ventricular Myocardial Perfusion Reserves Correlate With Right Ventricular Function and Pulmonary Hemodynamics in Patients With Pulmonary Arterial Hypertension," *Radiology* 258, no. 1 (2011): 119–127.
29. C. Vahdatpour, S. Epstein, K. Jones, et al., "A Review of Cardio-Pulmonary Microvascular Dysfunction in Pulmonary Hypertension," *American Heart Journal Plus: Cardiology Research and Practice* 26 (2023): 100255.
30. C. Fauvel, Y. Liu, P. Correa-Jaque, et al., "Do Patients With Low-Risk Pulmonary Arterial Hypertension Really Benefit From Upfront Combination Therapy?," *Chest* 164, no. 6 (2023): 1518–1530.
31. A. Boucly, L. Savale, X. Jaïs, et al., "Association between Initial Treatment Strategy and Long-Term Survival in Pulmonary Arterial Hypertension," *American Journal of Respiratory and Critical Care Medicine* 204, no. 7 (2021): 842–854.
32. R. Souza, D. B. Badesch, H. A. Ghofrani, et al., "Effects of Sotatercept on Haemodynamics and Right Heart Function: Analysis of the

STELLAR Trial,” *European Respiratory Journal* 62, no. 3 (2023): 2301107.

33. M. Riou, I. Enache, F. Sauer, A. L. Charles, and B. Geny, “Targeting Mitochondrial Metabolic Dysfunction in Pulmonary Hypertension: Toward New Therapeutic Approaches?,” *International Journal of Molecular Sciences* 24, no. 11 (2023): 9572.

34. K. Vasan, M. Werner, and N. S. Chandel, “Mitochondrial Metabolism as a Target for Cancer Therapy,” *Cell Metabolism* 32, no. 3 (2020): 341–352.

35. S. N. Avdeev, O. L. Barbarash, A. E. Bautin, et al., “2020 Clinical Practice Guidelines for Pulmonary Hypertension, Including Chronic Thromboembolic Pulmonary Hypertension,” *Russian Journal of Cardiology* 26, no. 12 (2021): 4683.

36. S. N. Avdeev, O. L. Barbarash, Z. S. Valieva, et al., “2024 Clinical Practice Guidelines for Pulmonary Hypertension, Including Chronic Thromboembolic Pulmonary Hypertension,” *Russian Journal of Cardiology* 29, no. 11 (2024): 6161.